Elemental engineering: Epitaxial uranium thin films

R. Springell,[1,*] B. Detlefs,[2] G. H. Lander,[2] R. C. C. Ward,[3] R. A. Cowley,[3] N. Ling,[3] W. Goetze,[3] R. Ahuja,[4] W. Luo,[4] and B. Johansson[4,5]

[1]*European Synchrotron Radiation Facility, BP 220, F-38043 Grenoble Cedex, France*
[2]*European Commission, JRC, Institute for Transuranium Elements, Postfach 2340, 76125 Karlsruhe, Germany*
[3]*Clarendon Laboratory, University of Oxford, Oxford, Oxon OX1 3PU, United Kingdom*
[4]*Department of Physics, Uppsala University, Box 530, SE-751 21 Uppsala, Sweden*
[5]*Division of Applied Materials Physics, Department of Materials and Engineering, Royal Institute of Technology (KTH), SE-10044 Stockholm, Sweden*

Epitaxial films of the well-known alpha (orthorhombic) structure and an unusual hcp form of uranium have been grown on Nb and Gd buffers, respectively, by sputtering techniques. In a 5000 Å film of α-U a charge-density wave has been observed, and its properties are different from those found in the bulk. The 500 Å hcp-U film has a c/a ratio of 1.90(1), which is unusually large for the hcp structure. Theoretical calculations show that this hcp form is metastable and predict that it orders magnetically.

The production of epitaxial films has led to the discovery of a variety of new electronic, magnetic, and structural phenomena. These effects have had a major impact on our understanding of fundamental physical properties and on the development of new devices.[1] The two-dimensional regime of thin films and interactions, both electronic and structural (strain effects), with the substrate can lead to properties which differ dramatically from those of the bulk. The majority of metallic single-crystal epitaxial films produced so far have belonged to the transition- or rare-earth-metal series. We report here the growth of epitaxial films of uranium, the first element containing 5f electrons of the actinide series, in both the bulk room temperature (α-U) orthorhombic phase, as well as the hexagonal-close-packed (hcp-U) structure, which does not exist in the bulk. Uranium and other light actinides show a variety of interesting properties,[2] from heavy-fermion superconductors to ferromagnets, so that the growth of thin films opens up many research opportunities.

The films were grown in a dedicated dc magnetron sputtering facility at Oxford University with UHV base pressure, *in situ* reflection high-energy electron-diffraction (RHEED) analysis, and substrate heating to 900 °C.[3] The substrates were commercially polished, single-crystal $Al_2O_3(11\bar{2}0)$ plates. Buffer layers of niobium were employed and were deposited on sapphire substrates at 800 °C.

Niobium (bcc) grows epitaxially in the [110] orientation on sapphire ($11\bar{2}0$) at elevated temperature and single domains are formed.[4] Uranium was sputtered at various substrate temperatures in an argon pressure of 5×10^{-3} mbar and a growth rate of $0.5-1$ Å/s. In an additional experiment, a buffer layer of 500 Å gadolinium was inserted between the niobium and uranium layers; hcp-Gd grows epitaxially in the [0001] orientation on niobium (110). All the samples were capped with a thin layer of Nb to preserve the uranium layer from atmospheric attack for *ex situ* experiments. The structures were determined using a Pan analytical x-ray MRD diffractometer in Oxford with a Cu x-ray tube system equipped with a monochromator and analyzer, together with a curved focusing mirror.

The epitaxial relationship derived from the x-ray experiments[5] is shown schematically in Fig. 1. The orthorhombic form of α-U grows very well on the (110) plane of Nb, and the orientation axes of the 5000 Å film are shown in Fig. 1. The lattice mismatches are given in percent as a function of the uranium lattice spacings. These are large enough to promote considerable interfacial strain in metallic systems[6,7] and, depending on the growth mode, this can result in grain boundaries, impurities, voids, or dislocations. However, these effects dominate only in the early stages of film growth up to thicknesses of some tens of monolayers.[8] For the 5000 Å sample studied here, the U lattice parameter in the growth direction is $d(110)_U = 2.57$ Å, which is exactly the same as the bulk. The mosaic spread as measured from the transverse scan through the U (110) reflection is 0.15° and the atomic volume of U=20.7 Å^3, as in the bulk. All experiments as a function of temperature were made at the
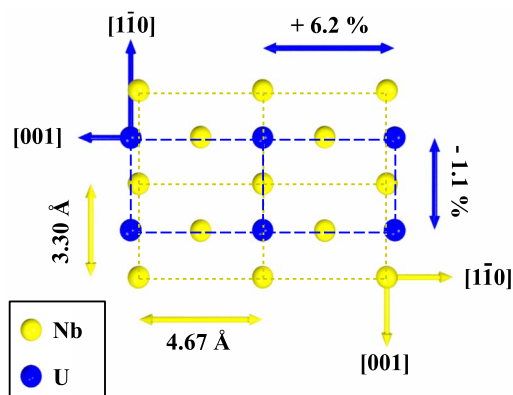

FIG. 1. (Color online) Two-dimensional projection illustrating the growth of the α-U epitaxial film (dashed lines are guides for the eyes). The initial substrate is single-crystal sapphire α-Al$_2$O$_3$, which is not shown. The Nb buffer (500 Å) (yellow spheres) has a growth axis [110], and one of the in-plane $[1\bar{1}1]$ axes is aligned parallel to the sapphire [0001]. The growth plane of α-U is (110) and the in-plane directions are shown.
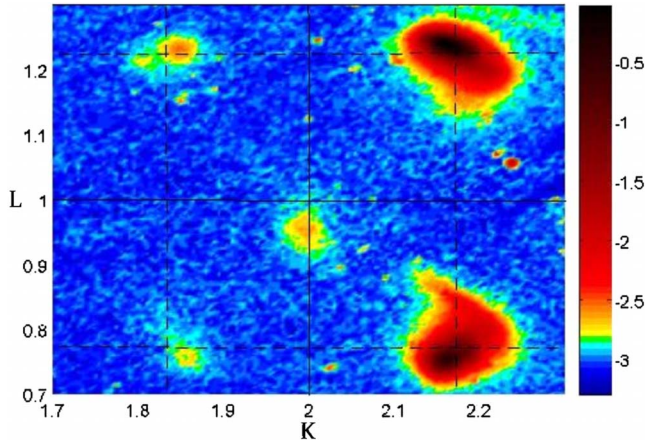
FIG. 2. (Color online) Plot of intensity (logarithmic scale) at $T=10$ K on the plane $(2.5\,K\,L)$ showing the four principal peaks from the CDW in the 5000 Å α-U film at the positions $(2.5\ \ K \pm q_y\ \ L \pm q_z)$, where $q_y=1/6$ and $q_z=2/9$. Note the large difference in intensity between the satellites at $(2.5\ 2^+\ 1^\pm)$ and those at $(2.5\ 2^-\ 1^\pm)$. The distortion of the peak shape of the strongest satellites is due to the weak fifth-order satellites that are identical in the K index and at 8/9 and 10/9 in the L index. The positions of the peaks are not exact because of alignment difficulties with such a large mesh; individual q values are obtained with line scans.

ID20 beamline at the European Synchrotron Radiation Facility (ESRF) in Grenoble[9] with an x-ray wavelength of 1.57 Å.

Bulk α-U exhibits a charge-density wave (CDW), initially at 43 K, and has been extensively characterized by both neutron and x-ray diffraction.[10] When the structural instability occurs due to the CDW, additional satellites appear in the diffraction pattern corresponding to new periodicies in the solid. In the case of α-U these new periodicies are found in all three directions in real space. A signature of the electron-phonon coupling that drives the CDW can be observed in the temperature dependence of the lattice parameters.[11] In the film a minimum in the d spacing is observed also, but it is smaller and more rounded than in the bulk, and occurs at a slightly lower temperature.

The search for the satellites arising from the CDW in the 5000 Å α-U film is summarized in the intensity contours shown in Fig. 2, which is a cut through the reciprocal lattice at the position $H=2.5$ with K and L varying. There are four main satellite peaks, grouped in pairs with similar intensities and equally spaced about the center point $\boldsymbol{Q}=[2.5\ 2\ 1]$. They represent the first-order satellites of the CDW, and are similar to those found in bulk samples.[10] From line scans, the individual components $[q_x\ q_y\ q_z]$ of the CDW wave vector $\boldsymbol{q}$ were deduced as a function of temperature and are compared to those found in the bulk[12] in Fig. 3. There are important differences between the CDW as found in the film and in the bulk:

(1) The large intensity difference (Fig. 2) between the $(2^+\ 2^+\ 1^\pm)$ and $(2^+\ 2^-\ 1^\pm)$ satellites shows that the domains with their propagation direction closer to the growth direction are strongly preferred. In a bulk sample,[10] intensity differences in this plane due to structure-factor effects do not exceed 40%.
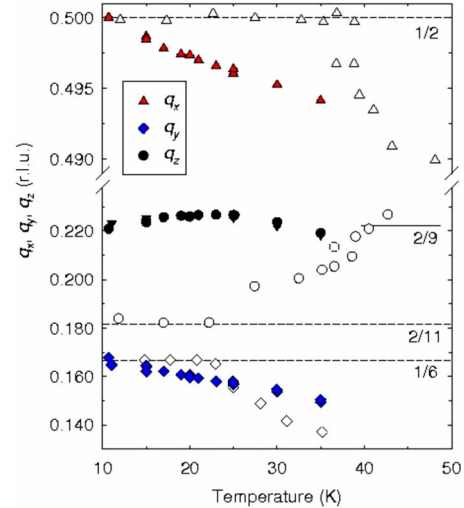

FIG. 3. (Color online) Components of the CDW wave vector $\boldsymbol{q}$ in the 5000 Å film of α-U as a function of temperature. The bulk values are indicated by open points and are taken from Ref. 12. Note that in the bulk there are lock-in transitions (where commensurate values are found that are independent of temperature) at $T=38$ K for q_x and 22 K for q_y and q_z. No lock-in transitions are observed in the film. The CDW disappears at 43 K in the bulk and at below 40 K in the film.

(2) Lock-in transitions, in which the q components take on commensurate values, are found in the bulk (Fig. 3); however, none are found in the film. This may be because the substrate clamps the film and prevents any elastic contribution to the energy. The CDW wave vector then varies smoothly with temperature and is controlled largely by the Fermi-surface nesting.[13]

(3) Further support for the quite different role of strain in the film compared to the bulk is the absence in the film of any measurable satellite at the "center" position $(q_x\ 0\ 0)$, which, in the bulk, is ascribed to finite domain walls of the CDW.[14] The signal in Fig. 2 at (2.5 2 0.95) is independent of temperature and spurious.

These experiments on the α-U film show that the details of the CDW are sensitive to a variety of external factors, but the overall distortion is driven by the strong electron-phonon interaction found in bulk α-U. An open question concerns dimensionality effects on the CDW as the film thickness is reduced.

Turning to other structures of uranium, we note that previous work[15,16] reported possibly stabilizing hcp-U as thin films (<100 Å) on W(110). We have tried to produce such films that can be characterized by x-ray diffraction. All attempts with W(110) have, so far, produced α-U films, although their domain arrangements are complex.[5] However, in our work on U/Gd multilayers[3] we observed that the uranium in these layers formed as hcp-U, although the lack of in-plane coherence prevented a determination of the in-plane a axis.

By inserting a 500 Å epitaxial Gd buffer on the Nb, we have succeeded in producing a 500 Å film of hcp uranium. As found for the U/Gd multilayers[3] the c axis is 5.625(5) Å, and measurements of the off-specular $(10\bar{1}4)$ reflection give
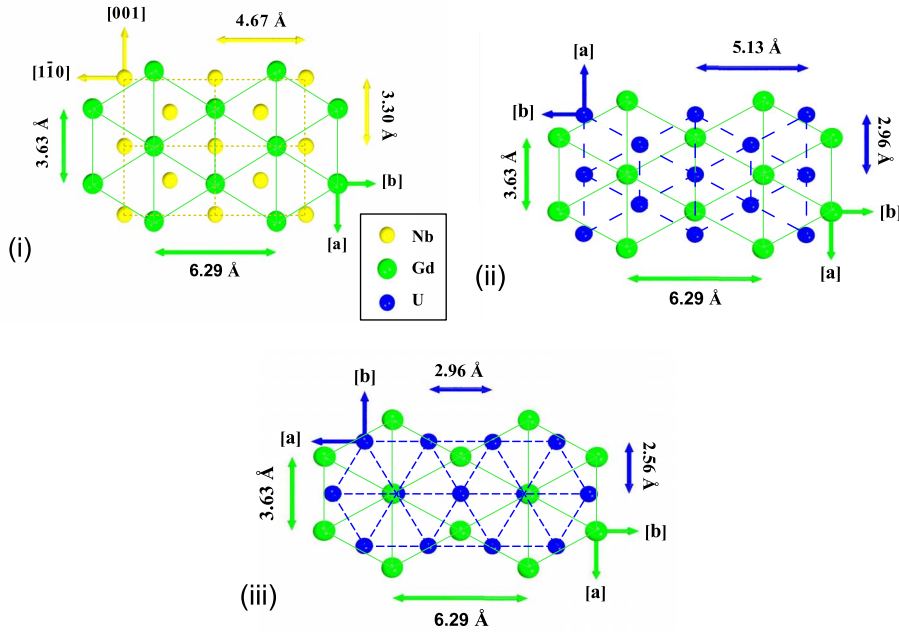
FIG. 4. (Color online) Growth characteristics of the hcp-U film. As in Fig. 1, the sapphire substrate is not shown. For the hexagonal systems (Gd and U) the in-plane orientations are denoted as $[a]$ and $[b]$, referring to $[11\bar{2}0]$- and $[\bar{1}100]$-type directions, respectively. (i) shows the growth of gadolinium on niobium, displaying the well-known 3Gd:4Nb relationship. (ii) and (iii) show the growth of hcp-U on Gd. We label the growth in (ii) domain 1, which has $[a]_U$ parallel to $[a]_{Gd}$ and a repeat motif every nine lattice spacings along $[a]_{Gd}$. (iii) Domain 2 is oriented at 30° to domain 1 and has $[b]_U$ parallel to $[a]_{Gd}$ and a repeat motif every seven lattice spacings along $[a]_{Gd}$.

$a=2.96(2)$ Å, compared to $c=5.784$ Å and $a=3.637$ Å for the Gd buffer. The respective atomic volumes are 21.3(2) Å^3 for hcp-U and 33.1 Å^3 for Gd. As expected, there is a six-fold repeat of the Gd off-specular reflections in the basal hexagonal plane, and the atomic volume is exactly as in the bulk. The in-plane mosaic is 0.6°, reflecting the relative misfit of Gd on Nb [see Fig. 4(i)], but it grows with one orientation only. For the hcp-U the atomic volume is expanded by ~3% as compared to α-U. However, the real surprise is the *almost 20% in-plane mismatch* between the closest U-U distance (2.96 Å) and that of Gd-Gd (3.637 Å). The large difference in the lattice parameters of U and Gd, shown schematically in Fig. 4, allows two different in-plane orientations of hcp-U to exist, rotated 30° to one another, giving rise to 12 reflections of almost equal intensity in plane, whereas normally one would expect only 6. The rocking curves of these reflections are large. We find ~1.5° for the hcp-U film, as compared to <0.2° for the α-U films on Nb, indicating a large mosaic spread, i.e., there is a large number of small domains of these two orientations.

To study the electronic structure of U, we have used the full-potential linear muffin-tin-orbital (FPLMTO) method.[17,18] The calculations were based on the generalized gradient approximation and we used the Perdew and Wang parametrization[19] for the exchange and correlation potential. The spin-orbit coupling was included explicitly. Basis functions, electron densities, and potentials were calculated without any geometrical approximation. These quantities were expanded in combinations of spherical harmonic functions (with a cutoff $l_{max}=6$) inside nonoverlapping spheres surrounding the atomic sites (muffin-tin spheres) and in a Fourier series in the interstitial region. The muffin-tin sphere occupied approximately 80% of the unit cell. The radial basis functions within the muffin-tin spheres are linear combinations of radial wave functions and their energy derivatives, computed at energies appropriate to their site and principal as well as orbital atomic quantum numbers, whereas outside the muffin-tin spheres the basis functions are combinations of Neuman or Hankel functions. In the calculations reported here, we made use of pseudocore 6s and 6p and valence band 7s, 7p, 6d, and 5f basis functions with corresponding two sets of energy parameters, one appropriate for the semicore 6s and 6p states, and the other appropriate for the valence states. The resulting basis formed a single, fully hybridizing basis set. This approach has been previously proven to give a well-converged basis.[20] For sampling the irreducible wedge of the Brillouin zone, we used the special k-point method with 512 k points in the irreducible part of the Brillouin zone. In order to speed up the convergence, we have associated each calculated eigenvalue with a Gaussian broadening of 20 mRy width. The total energy difference between the hcp and α-U phases was 0.21 eV/U atom.

To check the accuracy of our results for the hcp phase, we have first performed FPLMTO calculations for the α-U orthorhombic phase. Our calculations show that α-U is nonmagnetic. Once we reproduced the α-U phase, we went one step further and performed a fully relaxed structural calculation for hcp-U using the FPLMTO method. Our calculated c/a for hcp-U is 1.84 at an equilibrium volume of 21.22 Å^3/U. This compares well with the experimental values of 1.9 (c/a) and 21.3 Å^3/U (volume). Our calculations also show a small spin moment of ~0.1μ_B/U and an orbital moment of ~0.22μ_B/U aligned antiparallel. This small moment could be related to volume expansion or symmetry of the structure because under pressure the moment starts to reduce. We have done some preliminary calculations for the surface of the hcp phase and our results indicate that the spin moment is almost double compared to bulk hcp.

In summary, we have shown that α-U films can be grown relatively easily on Nb buffers deposited on sapphire. On cooling, the uranium phase diagram contains bcc-U$\rightarrow\beta$-U $\rightarrow\alpha$-U transformations, where the β phase is complicated.[21] Hence crystals of α-U are hard to produce: epitaxial films represent an alternative route. In a 5000 Å film we have

found the periodic distortions due to the CDW and there are differences between those found in this film and the bulk.[10] We shall be looking at thinner films and also search for the surface magnetism predicted in α-U.[22]

A characterized hcp-U epitaxial film of 500 Å has been produced, using a hcp-Gd buffer to stabilize this metastable phase of uranium. The dimensions of the unit cell (T =295 K) are c=5.625(5) Å and a=2.96(2) Å, giving a c/a=1.90(1). For hcp elements the largest values of c/a are found for Zn (1.86) and Cd (1.89), both of which have filled d shells. Thus, such a large value of c/a for uranium, which has a partially filled $5f$-electron shell, is unusual. Interestingly, the closest U-U distances (<3 Å) in α-U are ($2\times$) 2.75 and ($2\times$) 2.85 Å, whereas they are ($6\times$) 2.96 Å in hcp-U.

Whether the hcp-U has an electronic instability, leading to a possible CDW, or magnetic ordering, as predicted by the calculations above, awaits further experiments. With these technical developments of engineering thin epitaxial films of uranium, we have already stabilized a different form (hcp) and will attempt to grow films of the high-temperature bulk-like bcc structure. Theoretically, the three structures bcc $\rightarrow$hcp$\rightarrow\alpha$-U can be obtained by successively larger displacement of a TA[110] phonon in the bcc phase.[23] The ability to control the growth of such structures in uranium metal paves the way for new and exciting developments, addressing the role of $5f$ states in the structural stability of the light actinides.[24]

*ross.springell@esrf.fr

[1] *Ultrathin Magnetic Structures I: An Introduction to the Electronic, Magnetic and Structural Properties*, edited by J. A. C. Bland and B. Heinrich (Springer-Verlag, Berlin, 1994), Vol. 1.

[2] *Handbook on the Physics and Chemistry of the Actinides*, edited by A. J. Freeman and G. H. Lander (North-Holland, Amsterdam, 1984), Vol. 1.

[3] R. Springell, S. W. Zochowski, R. C. C. Ward, M. R. Wells, S. D. Brown, L. Bouchenoire, F. Wilhelm, S. Langridge, W. G. Stirling, and G. H. Lander, J. Phys.: Condens. Matter **20**, 215229 (2008); **20**, 215230 (2008).

[4] R. C. C. Ward, E. J. Grier, and A. K. Petford-Long, J. Mater. Sci.: Mater. Electron. **14**, 533 (2003).

[5] R. C. C. Ward, R. A. Cowley, N. Ling, W. Goetze, G. H. Lander, and W. G. Stirling, J. Phys.: Condens. Matter **20**, 135003 (2008).

[6] R. Koch, D. Winau, K. Thürmer, M. Weber, and K. H. Rieder, Europhys. Lett. **21**, 213 (1993).

[7] A. J. Schell-Sorokin and R. M. Tromp, Phys. Rev. Lett. **64**, 1039 (1990).

[8] R. Koch, D. Winau, and K. H. Rieder, Phys. Scr. **T49B**, 539 (1993).

[9] L. Paolasini *et al.*, J. Synchrotron Radiat. **14**, 301 (2007).

[10] G. H. Lander, E. S. Fisher, and S. D. Bader, Adv. Phys. **43**, 1 (1994).

[11] C. S. Barrett, M. H. Mueller, and R. L. Hitterman, Phys. Rev. **129**, 625 (1963).

[12] G. Grübel, J. D. Axe, D. Gibbs, G. H. Lander, J. C. Marmeggi, and T. Brückel, Phys. Rev. B **43**, 8803 (1991).

[13] L. Fast, O. Eriksson, B. Johansson, J. M. Wills, G. Straub, H. Roeder, and L. Nordström, Phys. Rev. Lett. **81**, 2978 (1998).

[14] Y. Yamada, Phys. Rev. B **47**, 5614 (1993).

[15] S. L. Molodtsov, J. Boysen, M. Richter, P. Segovia, C. Laubschat, S. A. Gorovikov, A. M. Ionov, G. V. Prudnikova, and V. K. Adamchuk, Phys. Rev. B **57**, 13241 (1998).

[16] L. Berbil-Bautista, T. Hänke, M. Getzlaff, R. Wiesendanger, I. Opahle, K. Koepernik, and M. Richter, Phys. Rev. B **70**, 113401 (2004).

[17] J. M. Wills and B. R. Cooper, Phys. Rev. B **36**, 3809 (1987).

[18] D. L. Price and B. R. Cooper, Phys. Rev. B **39**, 4945 (1989).

[19] J. P. Perdew and Y. Wang, Phys. Rev. B **45**, 13244 (1992).

[20] R. Ahuja, S. Auluck, J. M. Wills, M. Alouani, B. Johansson, and O. Eriksson, Phys. Rev. B **55**, 4999 (1997).

[21] A. C. Lawson, C. E. Olsen, J. W. Richardson Jnr, M. H. Mueller, and G. H. Lander, Acta Crystallogr., Sect. B: Struct. Sci. **44**, 89 (1988).

[22] N. Stojić, J. W. Davenport, M. Komelj, and J. Glimm, Phys. Rev. B **68**, 094407 (2003).

[23] J. D. Axe, G. Grübel, and G. H. Lander, J. Alloys Compd. **213–214**, 262 (1994).

[24] P. Söderlind, O. Eriksson, B. Johansson, J. M. Wills, and A. M. Boring, Nature (London) **374**, 524 (2002).